Thin Solid Films 518 (2010) 7328–7332

Contents lists available at ScienceDirect

Thin Solid Films

journal homepage: www.elsevier.com/locate/tsf

Photoresponse of hydrothermally grown lateral ZnO nanowires

Po-Yu Yang [a,*], Jyh-Liang Wang [b], Wei-Chih Tsai [c], Shui-Jinn Wang [c], Jia-Chuan Lin [d], I-Che Lee [a], Chia-Tsung Chang [a], Huang-Chung Cheng [a]

[a] Department of Electronics Engineering and Institute of Electronics, National Chiao Tung University, Hsinchu 30010, Taiwan
[b] Department of Electronics Engineering, Ming Chi University of Technology, Taipei 24301, Taiwan
[c] Institute of Microelectronics, Department of Electrical Engineering, National Cheng Kung University, Tainan 70101, Taiwan
[d] Department of Electronics Engineering, St. John's University, Taipei 25135, Taiwan

ARTICLE INFO

Available online 12 May 2010

Keywords:
Nanowire
Self-assembled lateral growth
Hydrothermal method
Low temperature

ABSTRACT

In this paper, a simple self-assembled lateral growth of ZnO nanowires (NWs) photodetector has been synthesized by a hydrothermal method at a temperature as low as 85 °C. The ZnO NWs exhibit single-crystalline wurtzite with elongated *c*-axis and can be selectively lateral self-assembled around the edges of ZnO seeding layer. The current of ZnO NWs is sensitive to the variation of ambient pressures, i.e. 4.47 μA was decreased to 1.48 μA with 5 V-bias as 1.1×10^{-6} Torr changed to 760 Torr, accordingly. Moreover, the current–voltage characteristics of ZnO NWs photodetectors can be evidently distinguished by UV illumination (i.e. λ = 325 nm). The photocurrent of ZnO NWs with UV illumination is twice larger than dark current while the voltage biased at 5 V. Consequently, this faster photoresponse convinces that the hydrothermally grown lateral ZnO NWs devices have a fairly good for the fabrication of UV photodetectors.

1. Introduction

ZnO nanowires (NWs) have attracted much attention as candidates for optoelectronic and electronic devices. ZnO NWs possess high surface-to-volume ratio, a direct energy wide-bandgap (i.e. ~3.37 eV) at room temperature, and a large exciton binding energy (i.e. ~60 meV). The potential uses of ZnO NWs as gas sensors, solar cells [1] and light emitting diodes [2] have been intensively explored. Recently, ZnO NWs have been investigated for UV photodetector applications [3–7]. The ZnO NWs were obtained by several techniques such as thermal evaporation [3], electron-beam lithography [4], chemical vapor deposition (CVD) [5], high growth temperature [6], and electric-field assisted assembly [7]. However, the reported techniques required complex and time-consuming manufacture and high temperature process, restricting the realistic mass fabrication of ZnO NWs optoelectronic devices.

In this paper, a simple hydrothermal method was adopted for ZnO NWs growth because of the advantages of low cost of equipment, large-area and uniform fabrication, catalyst-free growth, environmental friendliness, and low processing temperature. Thus, the low-temperature ZnO NWs were synthesized by hydrothermal method, and the related photoresponse characteristics of ZnO NWs are addressed and analyzed.

2. Experimental details

The schematic fabrication procedures of ZnO NWs photodetectors are shown in Fig. 1. The (100) oriented p-type Si wafers were used as the substrates for NW growth. After Standard RCA cleaning, a ZnO film (~200 nm) and Ti (~5 nm)/Pt (~50 nm) films were deposited on Si substrate by using a sputtering system at room temperature. The ZnO and Ti/Pt films were patterned by a lifting-off technique and acted as a seed layer and contact metal, correspondingly. The samples were dipped in 0.001 M H_3PO_4 and then immersed in the mixed growth solution at 85 °C for 180 min. The growth solution was prepared by mixing with 0.025 M zinc nitrate hexahydrate ($Zn(NO_3)_2\cdot6H_2O$) and 0.025 M hexamethylenetetramine (HMTA) in deionized water at

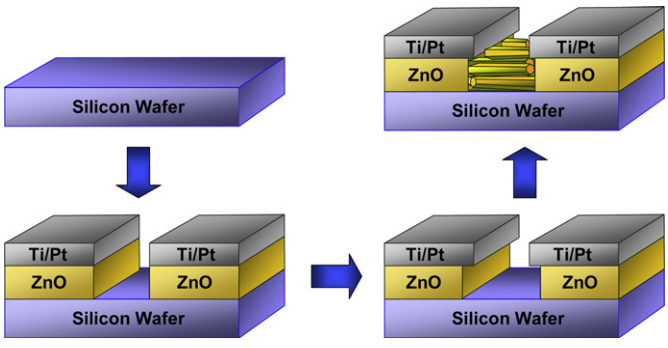

Fig. 1. The fabrication procedures of ZnO NWs photodetectors.

* Corresponding author. Lab. ED309B, Engineering Building 4, National Chiao Tung University, No. 1001, Ta Hsueh Rd., Hsinchu 30010, Taiwan.
E-mail address: youngboy.ee96g@g2.nctu.edu.tw (P.-Y. Yang).

0040-6090/$ – see front matter © 2010 Elsevier B.V. All rights reserved.
doi:10.1016/j.tsf.2010.04.104

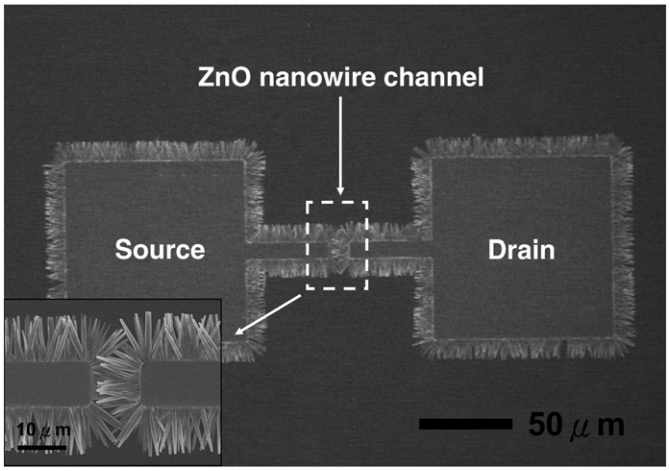

Fig. 2. Optical microscope image of the patterned device. The inset is an enlarged image of laterally self-assembled ZnO NWs with Ti/Pt electrodes.

room temperature. The illustrative equation of the possible chemical reactions during ZnO NWs formation in the aqueous solution can be expressed as following [8]

$$C_6H_{12}N_4 + 6H_2O \rightarrow 4NH_3 + 6HCHO \quad (1)$$

$$NH_3 + H_2O \Leftrightarrow NH_4^+ + OH^- \quad (2)$$

$$Zn^{2+} + 2OH^- \rightarrow ZnO + H_2O \quad (3)$$

Subsequently, the samples were thoroughly rinsed with deionized water in order to eliminate residual salts and dried in air at room temperature. The surface morphologies were observed by a field-emission scanning electron microscopy (FE-SEM, Hitachi S-4700I). The crystal structure of the ZnO NWs was confirmed using X-ray diffraction (XRD) by a diffractometer (M18XHF, MAC Science) with the incident radiation of Cu Kα ($\lambda = 0.154$ nm) and fixed 2θ scanning range of 30° to 60°. The crystallinity and chemical composition of the ZnO NWs were investigated using transmission electron microscopy (TEM, JEOL JEM-3000F) and energy-dispersive X-ray spectroscope (EDS). The TEM samples were prepared by scraping wires off the substrates, followed by dispersion in ethanol and then drop casted onto holey carbon coated copper grids. The optical emission properties of ZnO NWs were examined by photoluminescence (PL) spectra with He–Cd laser excitation, i.e. $\lambda = 325$ nm. Furthermore, the photocurrent of ZnO NWs photodetectors was characterized by a source measurement unit (Keithley 2400) with a monochromatic UV light source of Xe arc lamp, i.e. $\lambda = 325$ nm.

3. Results and discussion

The device morphology of ZnO NWs photodetector is shown in Fig. 2. The channel region of this photodetector is $10 \times 10\ \mu m^2$, and the

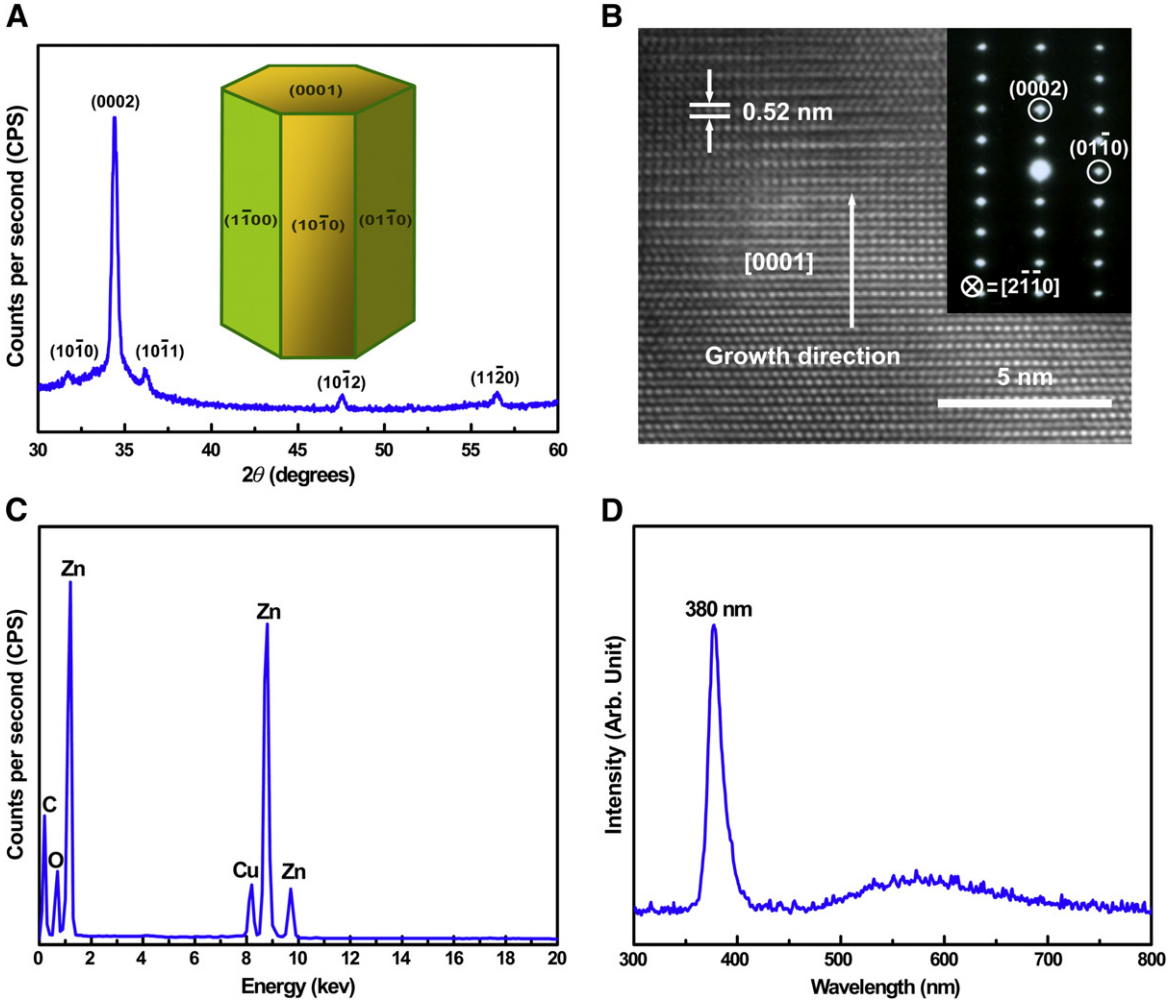

Fig. 3. (A) The X-ray diffraction patterns of ZnO NWs on ZnO/Si substrate. (B) A HRTEM lattice image of a ZnO NW. The inset shows the corresponding SAED pattern. (C) EDS analysis of a ZnO NW. (D) Photoluminescence spectra of ZnO NWs were measured at room temperature with the using an excited He–Cd laser (i.e. $\lambda = 325$ nm).

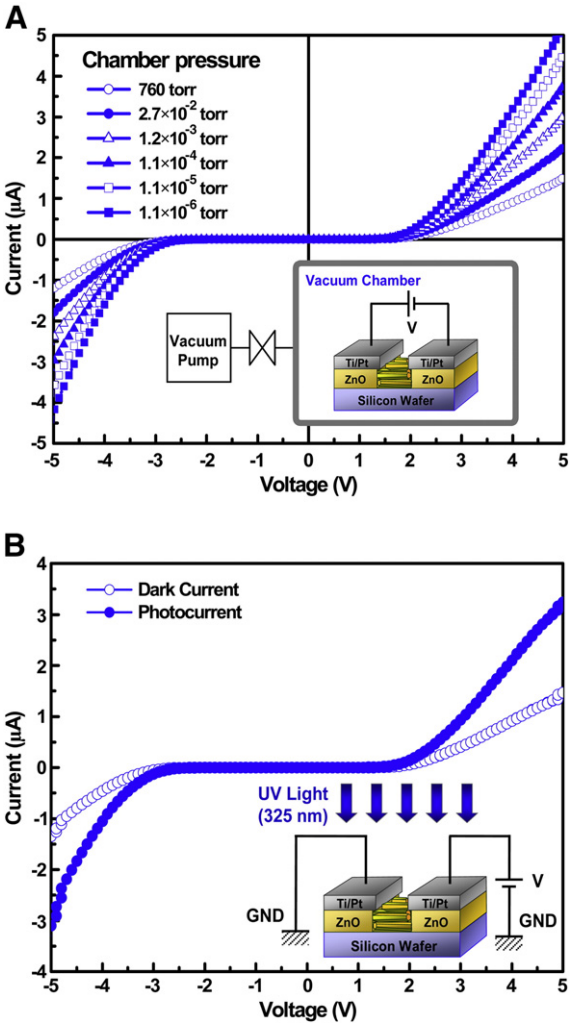

Fig. 4. (A) Current–voltage characteristics of ZnO NWs were studied for different chamber pressures at room temperature. (B) Current–voltage characteristics of ZnO NW photodetectors with and without UV illumination.

distance between the two electrodes is 10 μm. The selectively lateral self-assembled ZnO NWs grew and well-aligned around the edges of ZnO seeding areas. On the contrast, no NWs are observed on the electrodes of sputtered Ti/Pt. The inset of Fig. 2 presents the enlarged image of the device channel, indicating that the diameters of ZnO NWs are 50 nm–100 nm and the length of ZnO NWs can be approximate the spacing of two electrodes (i.e. ~10 μm), accordingly. Therefore, it evidences that the ZnO NWs can be uniformly-controlled grown and selectively lateral self-assembled around the edges of ZnO seeding layer.

Fig. 3A reveals the XRD pattern of ZnO NWs on ZnO/Si substrate. The diffraction peaks can be indexed to a wurtzite hexagonal structure of the ZnO crystal with lattice constants $a = 0.325$ nm and $c = 0.521$ nm. The relatively strong peak located at around 34.8° can correspond to the orientation of ZnO (0002) and infer that these nanostructures are well-aligned and oriented along [0001] direction, the *c*-axis of ZnO crystal, and perpendicular to the substrate. A TEM technique was also conducted to confirm the crystalline and orientation of the ZnO NWs. The high resolution transmission TEM (HRTEM) image shown in Fig. 3B clearly presents a well-resolved lattice with the measured inter-plane spacing of ~0.52 nm. Moreover, the growth direction of ZnO NWs was examined with both of HRTEM image and selective area electron diffraction (SAED) pattern (the inset of Fig. 3B) identified as along the [0001] direction, which is the fastest growth direction for ZnO crystals. Thus, the crystallinity and structure of ZnO NWs can be classified as single-crystalline wurtzite with elongated *c*-axis. In Fig. 3C, the feature peaks of EDS spectra can correlate to the signals of Zn and O, indicating that there is no additional impurity of metal element. The noise of Cu feature peaks came from the Cu grid used in TEM analysis. The PL investigation of ZnO has been extensively studied for the potential optical applications [9]. Fig. 3D demonstrates the room temperature PL spectra of ZnO NWs, indicating a strong UV peak and a broad green emission band. The UV peak centered at 380 nm (i.e. 3.26 eV) and can be linked to the near-band-edge (i.e. 3.37 eV) emission and free-exciton peak of ZnO [10]. The broad green bands of visible region located at ~570 nm (i.e. 2.18 eV) and can be related to native defect levels within the band gap, such as single and double ionized oxygen vacancies [11]. The sufficient Zn^{2+} and the slow release of OH^- from HMTA in the reaction solution lead to the lack of oxygen and form the oxygen vacancy of ZnO NWs while the ZnO NWs formation in the aqueous solution during hydrothermal method process [8].

Fig. 4A presents the current–voltage characteristics of ZnO NWs, measured for different chamber pressures at room temperature. The current decreased from 4.47 μA to 1.48 μA under the bias of 5 V as the chamber pressure increased from 1.1×10^{-6} Torr to 760 Torr, which might be correlated to the activities of surface defects on ZnO with ambience. The surface defects on ZnO, such as oxygen vacancies, can act as adsorption sites in the surface layer [12,13]. The adsorption of a

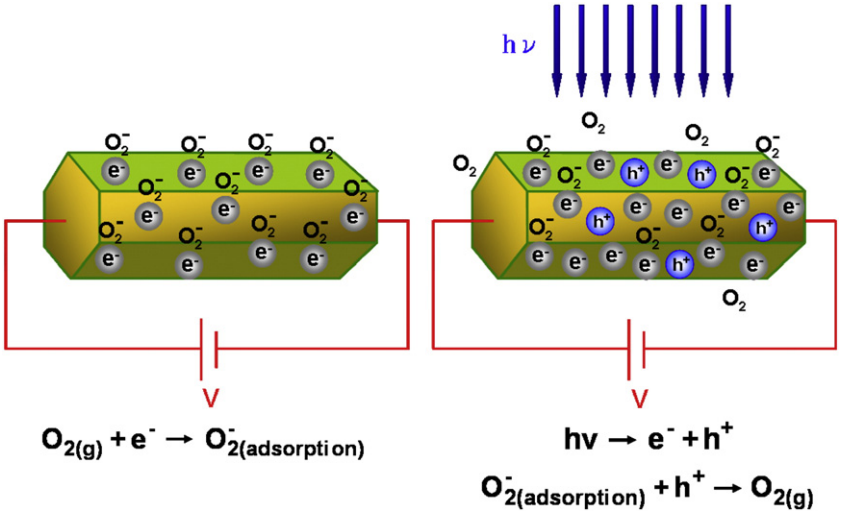

Fig. 5. Schematic diagram of photoconduction in ZnO NWs photodetectors.

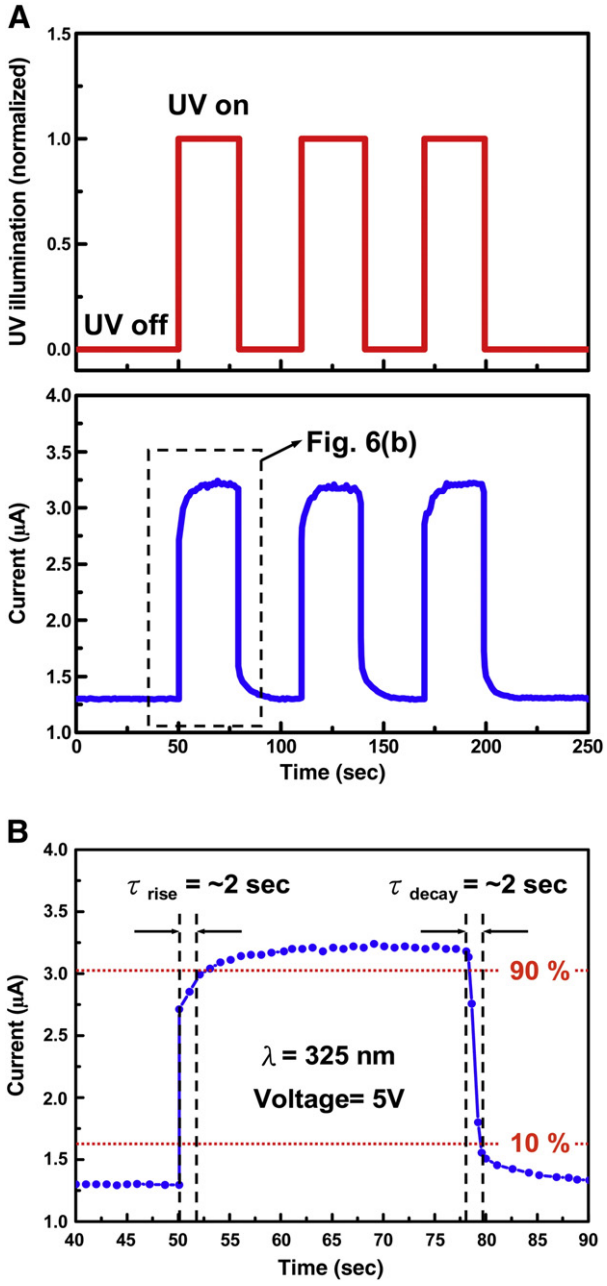

Fig. 6. (A) The Photoresponse of ZnO NWs photodetectors with and without UV illumination in the air. (B) The enlarged view of photoresponse.

gas molecule on the surface of ZnO NW, such as O_2 and H_2O, will trap the free electrons in the NW [14,15]. Therefore, the adsorbates performing as acceptors depleted the surface electron states and consequently reduced the conductivity while chamber pressure increased. The sensitive variation of current changed with the ambience implies that the self-assembled lateral growth ZnO NWs can be possibly used as pressure sensors. Fig. 4B indicates that the current–voltage characteristics of ZnO NWs photodetectors can be evidently distinguished by UV illumination. The nonlinear current–voltage characteristic might originate from the existence of barriers between the Ti/Pt electrodes and the ZnO NWs [16]. The photocurrent with UV illumination can be twice larger than dark current while the voltage biased at 5 V.

Normally, as-grown ZnO can be considered as an n-type semiconductor owing to the intrinsic defects, such as oxygen vacancies and Zn interstitials [17], which can be connected to the analysis of broad green bands in PL spectra (shown in Fig. 3D). The defects act as adsorption sites in the surface. As oxygen is adsorbed on the surface of ZnO NWs in the dark, it captures electrons from the NWs and forms negatively charged ions as following formulas [5]

$$O_{2(g)} + e^- \rightarrow O^-_{2(\text{adsorption})} \quad (4)$$

$$h\nu \rightarrow e^- + h^+ \quad (5)$$

$$O^-_{2(\text{adsorption})} + h^+ \rightarrow O_{2(g)} \quad (6)$$

Likewise, this process leads to the formation a space charge region and band bending upwards near the surface. When the ZnO NWs device is irradiated by a light with photon energy higher than the band gap, electron–hole pairs are generated. The photogenerated electron–hole pairs are separated in the space charge region, and then holes migrate to the surface along the bending band and react with negatively charged oxygen ions. Then, the photogenerated electrons increase the photocurrent due to the enhanced carrier density in the ZnO NWs. Fig. 5 illustrates the schematic mechanism for the chemical reactions of photoconduction in ZnO NW photodetectors.

Moreover, Fig. 6A reveals that the photoresponse of the ZnO NWs to UV (i.e. $\lambda = 325$ nm) illumination in air is as a function of irradiation time while the bias was sustained at 5 V. The reversible cycles of the photoresponse curve indicates a stable and repeatable operation of photo detecting and optical sensing. Fig. 6B shows the enlarged view of photoresponse. The rise time (defined as the time for the current to rise to 90% of the peak value) and decay time (defined as the time for the current to decay to 10% of the peak value) of hydrothermally grown lateral ZnO NWs photodetectors are extracted as ~2 s and ~2 s, accordingly. Table 1 summaries the UV photoresponse of ZnO NWs photodetectors in this work and the reported ZnO photodetectors in literatures [3–5,18,19], where the photoresponse of ZnO NWs-based, ZnO single NW-based, and film-based photodetectors are quantitatively compared. The photoresponse of reported ZnO photodetectors under UV illumination indicate a slow response, ranging from a few minutes to~1 h [3–5,18,19]. The UV photoconduction and carrier transport in these ZnO films depend on the grain size, thickness of film [20], orientation of crystallographic [21], and the presence of different

Table 1
UV photoresponse of ZnO NWs photodetectors in this work and the reported ZnO photodetectors in literatures.

	This study	[3]	[4]	[5]	[18]	[19]
Photodetector architecture	Nanowires	Nanowires	Single nanowire	Single nanowire	Thin film	Thin film
Crystalline	Single crystalline	Not available	Single crystalline	Single crystalline	Polycrystalline	Polycrystalline
Preparation method	Hydrothermal method	Thermal evaporation method	Hydrothermal method	Chemical vapor deposition method	Pulsed laser deposition method	RF magnetron sputtering method
Processing temperature (°C)	85	900	95	925	580	700
Rise time (s)	2	90	5.6	23	90	Not available
Decay time (s)	2	3500	Not available	33	900	600

amounts of defect concentration [22], resulting in the large variation of photoresponse times in reported studies. The relatively faster photoresponse in this work could be associated to the superior single-crystalline and increase photoactive areas using multi-nanowire-based architecture [23]. This faster photoresponse in this work convinces that the hydrothermally grown lateral ZnO NWs devices have a fairly good for the fabrication of UV photodetectors. The low-temperature hydrothermally grown ZnO NWs also disclosure the potentials applied in flexible optoelectronic devices.

4. Conclusions

A self-assembled lateral growth ZnO nanowires (NWs) photodetector was fabricated by hydrothermal method at a relatively low temperature, i.e. 85 °C. The ZnO NWs can be uniformly-controlled grown and selectively lateral self-assembled around the edges of ZnO seeding layer. The crystallinity and structure of ZnO NWs are classified as single-crystalline wurtzite with elongated *c*-axis. While the chamber pressure increased from 1.1×10^{-6} Torr to 760 Torr, the current of ZnO NWs decreased from 4.47 μA to 1.48 μA under the bias of 5 V. Furthermore, the current–voltage characteristics of ZnO NWs photodetectors can be evidently distinguished by UV illumination. The photocurrent of ZnO NWs with UV illumination (i.e. $\lambda = 325$ nm) is twice larger than dark current while the voltage biased at 5 V. The rise time and decay time of photoresponse are extracted as ~2 s. This faster photoresponse in this work convinces that the hydrothermally grown lateral ZnO NWs devices have a fairly good for the fabrication of UV photodetectors. In short, the low-temperature hydrothermally grown ZnO NWs disclosed the potential applications of pressure sensors and flexible optoelectronic devices.

Acknowledgements

The authors at NCTU thank the National Science Council of Republic of China for their support under contract no. 98-2218-E-009-004 and no. 96-2628-E-009-169-MY3. Thanks are also due to the Chung-Shan Institute of Science & Technology, the Nano Facility Center (NFC) in National Chiao Tung University and the National Nano Device Laboratory (NDL) for the technical supports.

References

[1] M. Law, L.E. Greene, J.C. Johnson, R. Saykally, P. Yang, Nat. Mater. 4 (2005) 455.
[2] S.J. Jiao, Z.Z. Zhang, Y.M. Lu, D.Z. Shen, B. Yao, J.Y. Zhang, B.H. Li, D.X. Zhao, X.W. Fan, Z.K. Tang, Appl. Phys. Lett. 88 (2006) 031911.
[3] Q.H. Li, T. Gao, Y.G. Wang, T.H. Wang, Appl. Phys. Lett. 86 (2005) 123117.
[4] S.E. Ahn, H.J. Ji, K. Kim, G.T. Kim, C.H. Bae, S.M. Park, Y.K. Kim, J.S. Ha, Appl. Phys. Lett. 90 (2007) 153106.
[5] C. Soci, A. Zhang, B. Xiang, S.A. Dayeh, D.P.R. Aplin, J. Park, X.Y. Bao, Y.H. Lo, D. Wang, Nano Lett. 7 (2007) 1003.
[6] L. Luo, Y.F. Zhang, S.S. Mao, L.W. Lin, Sens. Actuators A 127 (2006) 201.
[7] Harnack, C. Pacholski, H. Weller, A. Yasuda, J.M. Wessels, Nano Lett. 3 (2003) 1097.
[8] C.H. Ku, J.J. Wu, J. Phys. Chem. B 110 (2006) 12981.
[9] P. Yang, H. Yan, S. Mao, R. Russo, J. Johnson, R. Saykally, N. Morris, J. Pham, R. He, H. J. Choi, Adv. Funct. Mater. 12 (2002) 323.
[10] Z.K. Tang, G.K. Wong, P. Yu, Appl. Phys. Lett. 72 (1998) 3270.
[11] K. Vanheusden, W.L. Warren, C.H. Seager, D.R. Tallant, J.A. Voigt, B.E. Gnade, J. Appl. Phys. 79 (1996) 7983.
[12] V.E. Henrich, P.A. Cox, Surface Science of Metal Oxides, Cambridge University Press, Cambridge, UK, 1994.
[13] Y. Zhang, A. Kolmakov, S. Chretien, H. Metiu, M. Moskovits, Nano Lett. 4 (2004) 403.
[14] Q.H. Li, Q. Wan, Y.X. Liang, T.H. Wang, Appl. Phys. Lett. 84 (2004) 4556.
[15] Z. Fan, D. Wang, P.C. Chang, W.Y. Tseng, J.G. Lu, Appl. Phys. Lett. 85 (2004) 5923.
[16] Z.M. Liao, J. Xu, J.M. Zhang, D.P. Yu, Appl. Phys. Lett. 93 (2008) 023111.
[17] T. Yamamoto, H.K. Yoshida, Physica B 302–303 (2001) 155.
[18] X.G. Zheng, Q.Sh. Li, W. Hu, D. Chen, N. Zhang, M.J. Shi, J.J. Wang, L.Ch. Zhang, J. Lumin. 122–123 (2007) 198.
[19] M. Liu, H.K. Kim, Appl. Phys. Lett. 84 (2004) 173.
[20] Y. Takahashi, M. Kanamori, A. Kondoh, H. Minoura, Y. Ohya, Jpn. J. Appl. Phys. Part 1 33 (1994) 6611.
[21] D.H. Zhang, D.E. Brodie, Thin Solid Films 251 (1994) 151.
[22] H.Y. Kim, J.H. Kim, Y.J. Kim, K.H. Chae, C.N. Whang, J.H. Songand, S. Im, Opt. Mater. 17 (2001) 141.
[23] J.D. Prades, R.J. Diaz, F.H. Ramirez, L.F. Romero, T. Andreu, A. Cirera, A.R. Rodriguez, A. Cornet, J.R. Morante, S. Barth, S. Mathur, J. Phys. Chem. C 112 (2008) 14639.